ANTIOXIDANTS & REDOX SIGNALING
Volume 15, Number 2, 2011
© Mary Ann Liebert, Inc.
DOI: 10.1089/ars.2010.3520

Chronic Exposure to Sulfide Causes Accelerated Degradation of Cytochrome c Oxidase in Ethylmalonic Encephalopathy

Ivano Di Meo,[1] Gigliola Fagiolari,[2] Alessandro Prelle,[3] Carlo Viscomi,[1] Massimo Zeviani,[1] and Valeria Tiranti[1]

Abstract

Ethylmalonic encephalopathy (EE) is an autosomal recessive, invariably fatal disorder associated with mutations in *ETHE1*, a gene encoding a mitochondrial sulfur dioxygenase (SDO). The main consequence of the absence of Ethe1-SDO is the accumulation of sulfide (H_2S) in critical tissues, including colonic mucosa, liver, muscle, and brain. To make progress in the elucidation of the biochemical mechanisms leading to cytochrome c oxidase (COX) deficiency, we (i) generated tissue-specific conditional *Ethe1* knockout mice to clarify the different contributions of endogenous and exogenous H_2S production, and (ii) studied the development of H_2S-driven COX deficiency in *Ethe1*$^{-/-}$ mouse tissues and human cells. *Ethe1*$^{-/-}$ conditional animals displayed COX deficiency limited to the specific targeted tissue. The accumulation of H_2S over time causes progressive COX deficiency in animal tissues and human cells, which is associated with reduced amount of COX holoenzyme, and of several COX subunits, including mitochondrially encoded cytochrome c oxidase 1 (MTCO1), MTCO2, COX4, and COX5A. This reduction is not paralleled by consistent downregulation in expression of the corresponding mRNAs. Tissue-specific ablation of *Ethe1* causes COX deficiency in targeted organs, suggesting that failure in neutralizing endogenous, tissue-specific production of H_2S is sufficient to cause the biochemical defect but neither to determine a clinical impact nor to induce the biomarker profile typical of EE. The mechanism by which H_2S causes COX deficiency consists of rapid *heme a* inhibition and accelerated long-term degradation of COX subunits. However, the pleiotropic devastating effects of H_2S accumulation in EE cannot be fully explained by the sole defect of COX in critical tissues, but are likely consequent to several toxic actions on a number of enzymatic activities in different tissues, including endothelial lining of the small vessels, leading to multiorgan failure. *Antioxid. Redox Signal*. 15, 353–362.

Introduction

ETHYLMALONIC ENCEPHALOPATHY (EE; OMIM No. 602473) is an autosomal recessive fatal infantile disease caused by accumulation of sulfide, H_2S, a mitochondrial poison produced exogenously by the anaerobic enterobacterial flora and synthesized endogenously in various mammalian tissues. Failure to detoxify sulfide is due to the absence or malfunctioning of a mitochondrial sulfur dioxygenase (SDO), encoded by the *ETHE1* gene, which is mutated in EE (30).

EE has been reported in numerous infants of Mediterranean or Arab origin who are clinically characterized by (i) progressive encephalopathy; (ii) chronic diarrhea; and (iii) petechial purpura and severe orthostatic acrocyanosis. Biochemically, EE presents an unusual combination of severe deficiency of cytochrome c oxidase (COX), the last component (complex IV, cIV) of the mitochondrial respiratory chain (RC), in both muscle and brain, accumulation in blood of C4 and C5 acylcarnitines and urinary excretion of ethylmalonic acid, the dicarboxylic derivative of butyrate (3). We found that the *ETHE1* gene codes for an SDO of the mitochondrial matrix, being part of a mitochondrial oxidative pathway for inorganic sulfur that ultimately converts sulfide into harmless compounds, such as thiosulfate and sulfate. This pathway is composed of four enzymes. First, a membrane-bound mitochondrial sulfide quinone reductase is involved in the initial oxidation of H_2S and the fixation of its sulfur atom to a sulfur acceptor, with the formation of a persulfide (12). Next, the persulfide compound is further oxidized to sulfite by molecular oxygen through the action of ETHE1-SDO. The enzyme rhodanese, which displays a sulfur transferase activity, acts in

[1]Unit of Molecular Neurogenetics, Pierfranco and Luisa Mariani Center for Research on Children's Mitochondrial Disorders, Institute of Neurology "Carlo Besta"–IRCCS Foundation, Milan, Italy.
[2]Division of Neurology, Dino Ferrari Center, Ospedale Maggiore Policlinico, Cà Granda-IRCCS Foundation, Milan, Italy.
[3]Neuroscience Department, Azienda Ospedaliera Fatebenefratelli e Oftalmico, Milan, Italy.

the third step, allowing sulfite to be trans-sulfurated in the mitochondrial matrix and converted into a metabolic end product, thiosulfate (12). Alternatively, sulfite can also be directly oxidized to sulfate by another mitochondrial matrix enzyme, sulfite oxidase. Wilson *et al.* (32) have proposed that yet another enzyme, sulfide oxidase, is active in the colonic mucosa, where it catalyzes the first and rate-limiting step of local sulfide catabolism, consisting of the oxidation/condensation of two molecules of H_2S to thiosulfate (H_2SO_3). Thiosulfate would then react with cyanide, being ultimately converted into thiocyanate by the trans-sulfurase activity of rhodanese. However, the very existence of sulfide oxidase has not been demonstrated, whereas *in vivo* experiments (11) have clearly shown that hardly any cyanide is produced in the large intestine, either by the mucosal cells or by the bacterial flora. Consequently very little, if any, thiosulfate can be converted into thiocyanate *in vivo*, casting doubt that this pathway exists *in vivo*. In any case, the consequence of impaired ETHE1 activity is the accumulation of sulfide, a harmful, biologically active compound that at micromolar concentrations acts as a powerful inhibitor of both COX and short-chain acyl-CoA dehydrogenase and possibly other enzymatic activities as well, damage the mucosa of the large intestine and endothelia, and alter the vessel tone, thereby accounting for the main clinical and biochemical features of EE. H_2S, together with NO and CO, belongs to a family of biological mediators termed gasotransmitters. H_2S exerts a host of biological actions on various targets, resulting in responses that range from cytotoxic to cytoprotective effects (27). Taken together, these data suggest that, in *Ethe1*$^{-/-}$ mice as in EE patients, low COX activity in muscle and in brain is due to the toxic accumulation of H_2S. We have previously shown that the biochemical defect of COX activity is paralleled in both tissues by concordant reduction in the steady-state amount of COX holoenzyme, suggesting that persistent inhibition of COX activity can induce its structural destabilization and accelerated degradation.

Besides endogenous production from catabolism of cysteine and other sulfur organic compounds, a substantial amount of H_2S derives from the anaerobic bacterial flora residing in the lumen of the large intestine (23). Similar to the EE intestinal lesions, excessive production and absorption of H_2S, combined with its reduced detoxification by colonocytes, are thought to play an important role in the mucosal damage of ulcerative colitis. To understand the contribution of exogenous *versus* endogenous H_2S production, we have characterized the phenotype of conditional *Ethe1*$^{-/-}$ mice in extraintestinal organs, namely, liver, brain, and skeletal muscle.

In addition, we investigated the consequences on COX of chronic exposure to H_2S in the *Ethe1*$^{-/-}$ mouse model, and in cultured human cells.

Materials and Methods

Cell lines, culture conditions, and treatments

Human primary fibroblasts and HeLa cells were grown in Dulbecco's modified Eagle's medium (DMEM) supplemented with 10% fetal bovine serum at 37°C in 5% CO_2 atmosphere. The cells were cultured without or with increasing concentrations (0.1–0.5 m*M*) of sodium hydrosulfide (NaHS; Sigma) freshly dissolved in the culture medium.

Creation and characterization of brain-, muscle-, and liver-specific conditional Ethe1$^{-/-}$ *mice*

Recombinant *Ethe1*$^{-/-}$ mice were obtained as described (30). A neomycin resistance cassette flanked by frt sites was removed by crossing with an *Flpe* transgenic mouse (16), thus obtaining *Ethe1*$^{+/LoxP}$ mice. The *Ethe1*$^{+/LoxP}$ animals were mated with three different transgenic strains expressing the *Cre* recombinase under (i) the liver-specific *Albumin* (21), (ii) the muscle-specific *MyoD* (4), and (iii) the brain-specific *Nestin* (31) promoters. *ETHE1*$^{+/LoxP,Cre}$ were eventually crossed with *Ethe1*$^{LoxP/LoxP}$ to obtain *Ethe1*$^{LoxP/LoxP,\ Cre}$ individuals.

Animals were euthanized at postpartum day 90 (P90) and the absence of the *Ethe1* gene and protein was verified in the tissues of each conditional model by PCR-based diagnosis on genomic DNA, and Western blot analysis with a specific a-ETHE1 antibody. Biochemical evaluation of complex IV activity was measured in muscle, brain, and liver homogenates. The measurement of thiosulfate in urine was performed as previously described (25).

Immunoblotting

Western blot analysis was performed with α-ETHE1 (28), α-cytochrome c oxidase subunit 1 (α-MTCO1) (1 μg/ml), subunit 2, α-MTCO2 (1 μg/ml), subunit 4, α-COX4 (0.5 μg/ml), subunit 5A, α-COX5A (1 μg/ml), α-succinate dehydrogenase-A (α-SDH-A; 0.1 μg/ml), α-Rieske iron–sulfur protein (RISP) (0.5 μg/ml), and α-NADH dehydrogenase (ubiquinone) 1 alpha subcomplex, 9 (α-NDUFA9) (0.5 μg/ml) (Invitrogen) antibodies, using the ECL chemiluminescence kit (Amersham), as described elsewhere (29).

Cells lysates were prepared from cells cultured in T-25 cm^2 flasks and resuspended in 3-(N-morpholino)propanesulfonic acid–sucrose buffer. Digitonin (0.2 mg/ml) was added and incubation was carried out on ice for 5 min. After centrifugation at 5000 *g* for 3 min, the pellet was resuspended in 1 m*M* EDTA, 3-(N-morpholino)propanesulfonic acid–sucrose buffer. After a second 5-min incubation on ice, cells were centrifuged at 10,000 *g* for 3 min. The pellet was resuspended in RIPA buffer (Tris-HCl 50 m*M* [pH 7.5], NaCl 150 m*M*, EDTA 5 m*M*, NP40 1%, and sodium deoxycholate 0.5%) plus protease inhibitors and incubated on ice for 30 min. Soluble proteins were separated from insoluble material by centrifugation at 18,000 *g* for 20 min. Mouse tissues were homogenized in 10×(v/w) of 10 m*M* potassium phosphate buffer (pH 7.5). Mitochondrial-enriched fractions were collected after centrifugation at 800 *g* for 10 min in the presence of protease inhibitors, and frozen and thawed twice in liquid nitrogen.

Approximately 60 μg of proteins was used for each sample in denaturing sodium dodecyl sulfate–polyacrylamide gel electrophoresis.

Real-time quantitative PCR

Total RNA was extracted from cells using RNeasy Mini Kit (Quiagen) according to the manufacturer's protocol. Tissue-derived RNA was isolated with TRIzol reagent (Invitrogen). Two micrograms of total RNA was treated with RNase-free DNase and retrotranscribed by using the Cloned AMV First-strand cDNA Synthesis kit and protocol (Invitrogen). Approximately 2–5 ng of cDNA was used for SYBR-GREEN based real-time PCR using primers specific for amplification

of several COX-subunit encoding genes according to ABI-Primer Express software; standard transcripts *HPRT* and *GAPDH* were co-amplified using suitable primers (see Supplementary Table S1). Real-time quantitative PCR was carried out using an ABI PRISM 7000 Sequence Detection System. The amplification profile was according to a two-step protocol: 1 cycle at 50°C for 2 min, 1 cycle at 95°C for 10 min, and then 40 cycles of 95°C for 15 s, and 60°C for 1 min. A final dissociation step (95°C for 15 s, 60°C for 20 s, and 95° for 15 s) was added to assess for unspecific primer–dimer amplifications.

Morphological and biochemical analyses

For light microscopy, samples from different tissues were frozen in liquid-nitrogen-cooled isopentane. Standard histological and histochemical techniques for the detection of mitochondrial alterations and muscle fiber distribution were performed on serial cryostat cross sections as previously described.

Standard histochemical method for the detection of SDH activity on 8-μM-thick cryostat sections was followed by dissolving 3.2 m*M* phenazine methosulfate, 12 m*M* succinic acid, and 1.2 m*M* nitro blue tetrazolium (NBT) in 10 ml of 0.1 *M* phosphate buffer (pH 7.4). The pH of this incubation solution was adjusted to 7.6 and filtered through a Whatman No. 1 filter paper. Sections were incubated for 30 min at 37°C and then rinsed three times, 5 min each in distilled water at room temperature, and then mounted on glass slides with warm glycerin. In some SDH reactions, the following compounds were added: 10 m*M* Na malonate or 1 m*M* NaHS.

Standard histochemical reaction on cryostat sections for COX was performed as described (24). For COX+SDH double staining, the COX reaction was performed first, followed by the SDH reaction after rinsing the sections three times for 5 min each in distilled water.

Biochemical assays of the individual mitochondrial RC complexes and of citrate synthase (CS) on tissues and cells were carried out as described (2). The specific activities of each complex were normalized to CS, an indicator of the number of mitochondria. COX activity was evaluated in the homogenates incubated with 10 m*M* NaHS after addition of COX reaction mixture. The first measurement was performed within 2 min and then repeated every 10 min for 1 h. COX activity was recorded in parallel in untreated homogenates. Residual activity in treated samples was calculated as percentage of the normal activity measured in untreated homogenates.

In vivo *mitochondrial translation assay*

Mitochondrial protein synthesis was analyzed according to Chomyn (6) with some modifications. For the "pulse" experiment, cells at 70% confluence in T25 flasks were cultured for 24 h in the presence or absence of 0.5 m*M* NaHS and then incubated for 2 h with 100 μg/ml of emetine, an irreversible inhibitor of cytosolic protein synthesis, in the presence of 160 μCi/ml of [^{35}S]-Met/Cys (Express Protein Labeling Mix; Perkin Elmer) in methionine and cysteine-deficient DMEM. For the "chase" experiment, cells were preincubated with 40 μg/ml chloramphenicol for 15 h. Cells were then labeled for 2 h in the presence of 100 μg/ml cycloheximide, and further incubated in complete medium for 24 h, with or without 0.5 m*M* NaHS.

After washing and harvesting, cells were kept at −80°C until use. An equal amount of total cellular proteins was loaded on a 15%–20% exponential gradient sodium dodecyl sulfate–polyacrylamide gel electrophoresis. The gel was then fixed, dried, and autoradiographed using a PhosphorImager apparatus (BioRad).

Results

Evaluation of brain-, muscle-, and liver-specific conditional Ethe1$^{-/-}$ mice

Absence of the *Ethe1* gene and protein in liver-specific albumin, muscle-specific myoD, and brain-specific nestin conditional animals was verified by PCR (not shown) and Western blot analyses (Fig. 1A). The muscle homogenate of the myoD-specific and the brain homogenate of the nestin-specific conditional knockout animals both showed a 50%–60% isolated reduction of the COX activity, whereas neither the brain of the former nor the muscle of the latter animals showed the defect (Fig. 1B). In contrast, COX activity was normal in the liver, muscle, and brain of the liver-specific *Ethe1*$^{-/-}$ animals (Fig. 1B).

None of the three conditional mouse models showed the clinical and biological hallmarks of EE, at least for the period of our observation (90 days). In particular, urinary thiosulfate levels were comparable between conditional and wild-type (WT) animals (Fig. 1C).

Histochemical staining of Ethe1$^{-/-}$ constitutive animals

Constitutive *Ethe1*$^{-/-}$ mice are characterized by a downhill clinical course, which, starting at around P14, that is, the weaning time, leads the animals invariably to death within 30–35 days after birth. Severe COX deficiency is detected in the brain and muscle of P30 *Ethe1*$^{-/-}$ mice by both histochemical and biochemical assays. To understand if the onset of the clinical deterioration at P14 coincides with the onset and progression of COX deficiency, we analyzed histochemically the muscle, brain, and colon of P14, P21, and P30 *Ethe1*$^{-/-}$ mice. In muscle, COX deficiency progressed from mild reduction at P14 to severe reduction at P21, which further worsened in the terminal stage, at P30 (Fig. 2). The same progression was found in brain tissue (Fig. 3).

Examination of the intestinal tract showed diffuse, mild reduction of COX activity in the jejunal mucosa (not shown). In colonic mucosa, COX deficiency at P14 was limited to the colonocytes located on the luminal surface. Over time, COX deficiency progressively diffused from the luminal surface through the internal part of the mucosa to reach the deeper segments of the Lieberkhün crypts (Fig. 4). In all three tissues, that is, muscle, brain, and colon, we found a parallel strong increase in the histochemical reaction used to observe the activity of SDH, which is part of complex II (Figs. 1–3). This reaction is based on the capacity of SDH to reduce tetrazolium, a colorless salt, into formazan, a blue dye, in the presence of succinate. A hyperintense SDH reaction is typical of conditions characterized by proliferation of mitochondria, for example, ragged-red fibers in mitochondrial myopathies, and is accompanied by increased biochemical activities of SDH and CS, another index of mitochondrial mass, in tissue homogenate. However, neither SDH nor CS enzymatic activities

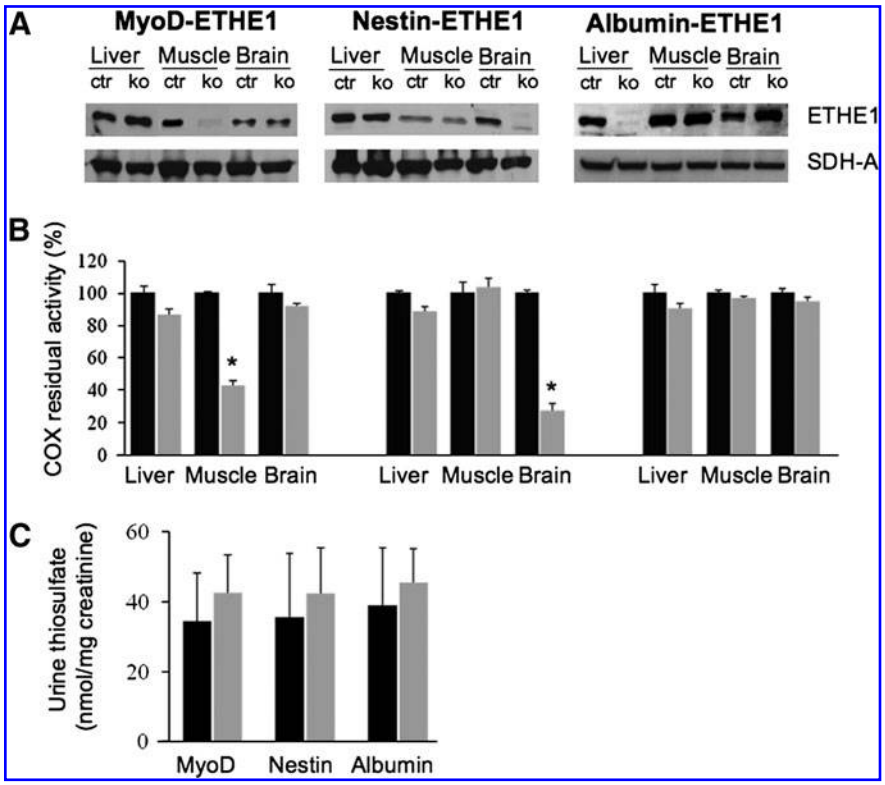

FIG. 1. Analysis of conditional *ETHE1*$^{-/-}$ animals. (A) Western blot assay using an α-ETHE1 antibody in different tissues of muscle-specific (MyoD), brain-specific (nestin), and liver-specific (albumin) *Ethe1*$^{-/-}$ mice. An α-SDH-A antibody was used as a protein-loading standard. **(B)** COX activity in different tissues of MyoD, nestin, and albumin-conditional *Ethe1*$^{-/-}$ mice. Black bars: control animals; gray bars: *Ethe1*$^{-/-}$ animals. **(C)** Thiosulfate concentration in the urine of MyoD, nestin, and albumin conditional *Ethe1*$^{-/-}$ mice. Blue bars: control animals; red bars: *Ethe1*$^{-/-}$ animals. COX, cytochrome c oxidase.

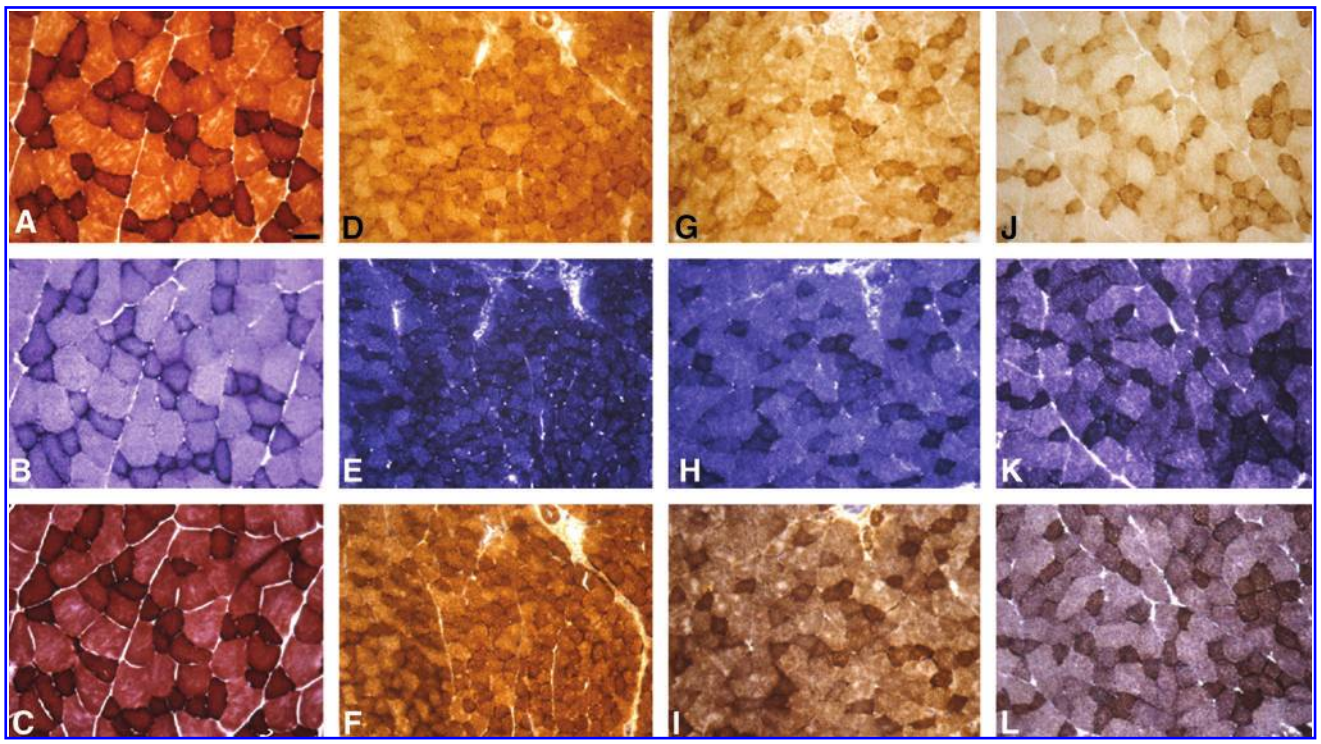

FIG. 2. Muscle histochemistry of constitutive *Ethe1*$^{-/-}$ mice. Muscle serial sections, scale bars: 20 μm. COX activity in WT animals **(A)**; *Ethe1*$^{-/-}$animals at P14 **(D)**, P21 **(G)**, and P30 **(J)**. SDH activity in WT animals **(B)**; *Ethe1*$^{-/-}$animals at P14 **(E)**, P21 **(H)**, and P30 **(K)**. COX-SDH double-stain in WT animals **(C)**; *Ethe1*$^{-/-}$animals at P14 **(F)**, P21 **(I)**, and P30 **(L)**. SDH, succinate dehydrogenase; WT, wild type. (To see this illustration in color the reader is referred to the web version of this article at www.liebertonline.com/ars).

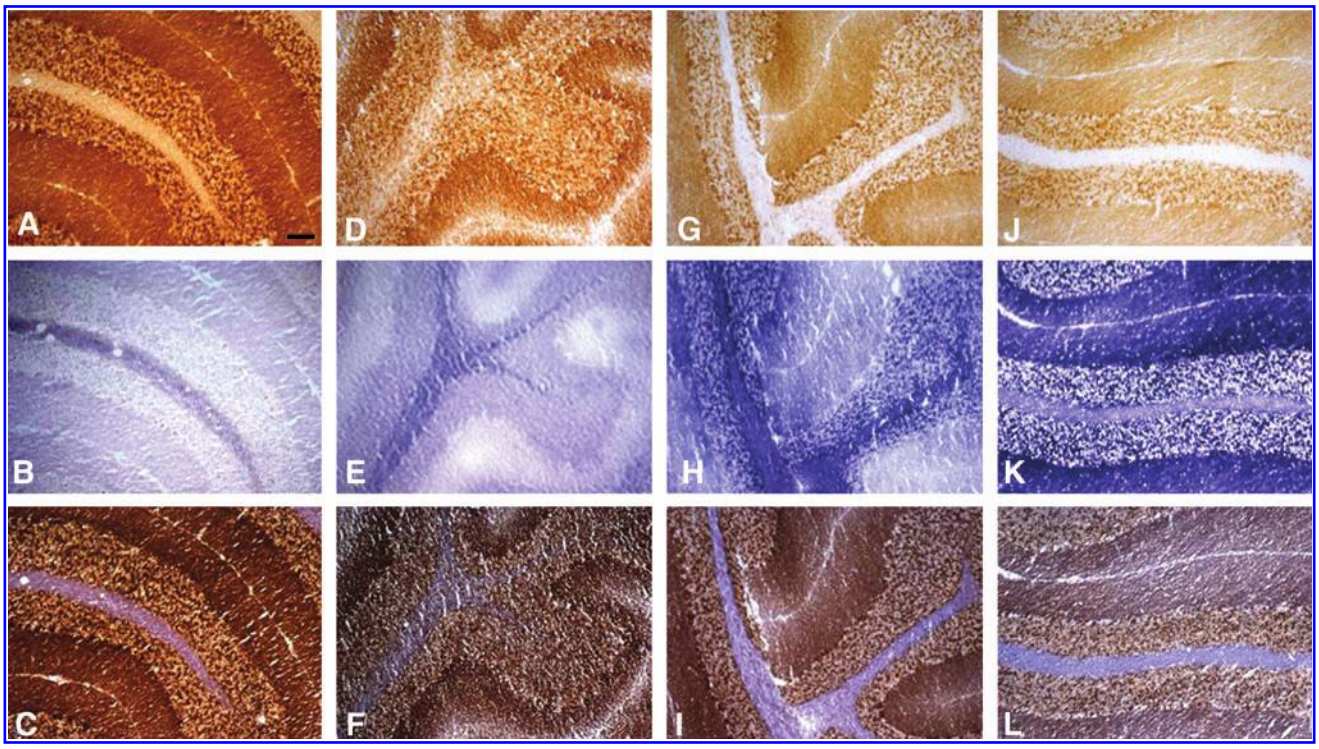

FIG. 3. Brain histochemistry of constitutive *Ethe1*$^{-/-}$ mice. Brain serial sections, scale bars: 50 μm. COX activity in WT animals **(A)**; *Ethe1*$^{-/-}$animals at P14 **(D)**, P21 **(G)**, and P30 **(J)**. SDH activity in WT animals **(B)**; *Ethe1*$^{-/-}$animals at P14 **(E)**, P21 **(H)**, and P30 **(K)**. COX-SDH double-stain in WT animals **(C)**; *Ethe1*$^{-/-}$animals at P14 **(F)**, P21 **(I)**, and P30 **(L)**. (To see this illustration in color the reader is referred to the web version of this article at www.liebertonline.com/ars).

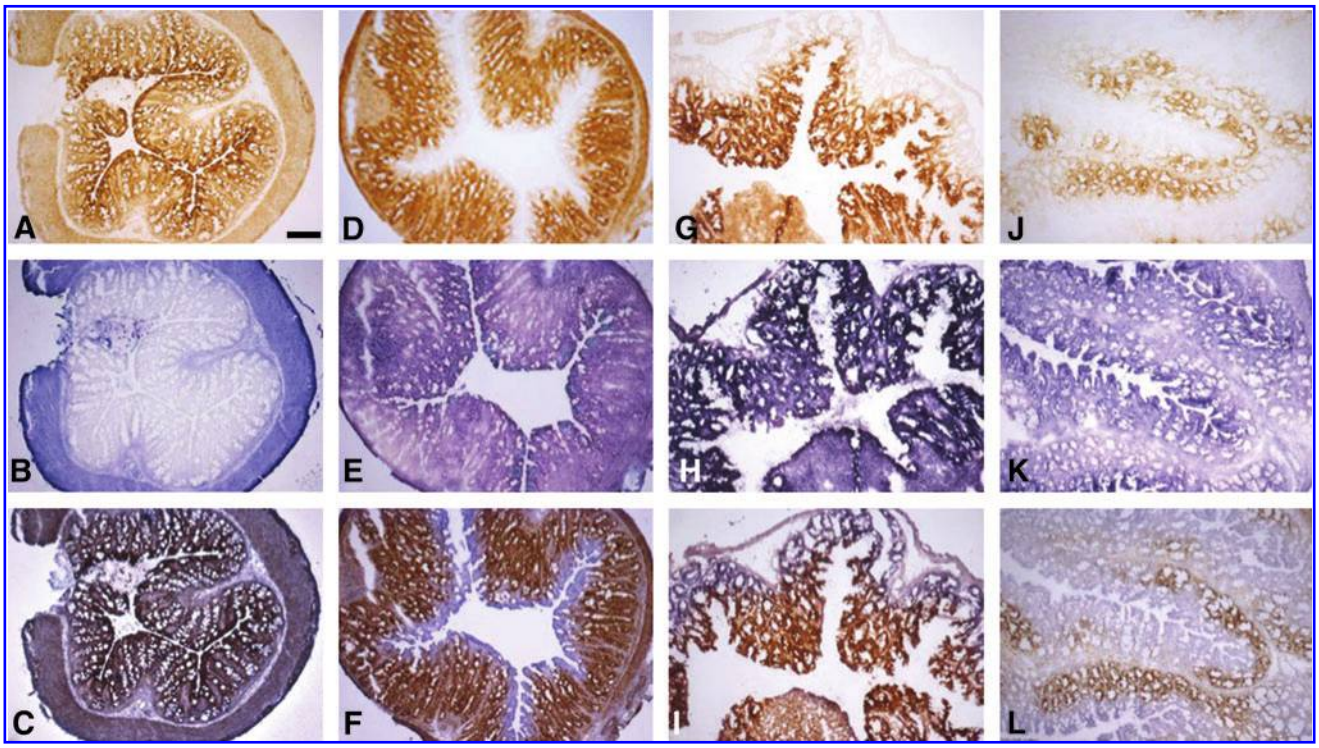

FIG. 4. Colon histochemistry of constitutive *Ethe1*$^{-/-}$ mice. Colon serial sections, scale bars: 50 μm. COX activity in WT animals **(A)**; *Ethe1*$^{-/-}$animals at P14 **(D)**, P21 **(G)**, and P30 **(J)**. SDH activity in WT animals **(B)**; *Ethe1*$^{-/-}$animals at P14 **(E)**, P21 **(H)**, and P30 **(K)**. COX-SDH double-stain in WT animals **(C)**; *Ethe1*$^{-/-}$animals at P14 **(F)**, P21 **(I)**, and P30 **(L)**. (To see this illustration in color the reader is referred to the web version of this article at www.liebertonline.com/ars).

were increased in *Ethe1*$^{-/-}$ tissue homogenates, nor was proliferation of mitochondria detected by ultra-structural studies (not shown), suggesting that the strong blue staining obtained histochemically was not due to increased SDH activity and mitochondrial proliferation, but rather to the presence of direct, nonenzymatic conversion of tetrazolium into formazan by H_2S and its persulfide derivatives (15). To test this hypothesis, we first incubated 1 m*M* of NaHS with 0.1 m*M* NBT in a test tube and verified that NBT was indeed reduced, by reading absorbance at 412 nm with spectrophotometric analysis. We then exposed WT muscle sections to 1 m*M* NaHS, which dissociates to Na^+ and HS^- in solution. HS^- then associates with H^+ and produces H_2S. At pH 7.4, in which the SDH reaction has been carried out, approximately one-third of the H_2S exists as the un-dissociated form (H_2S), the remaining two-thirds being present as HS (22). To avoid evaporation, the reactions were performed in chamber slides with a sealed cover.

While the standard SDH reaction gave a normal staining in the muscle of *Ethe1*$^{+/+}$ animals (Fig. 5A), a strong reaction was present in both NaHS-treated *Ethe1*$^{+/+}$ (Fig. 5B) and untreated *Ethe1*$^{-/-}$ muscles (Fig. 5C), Next, we treated muscle sections of *Ethe1*$^{+/+}$ and *Ethe1*$^{-/-}$ animals with (i) malonate, a specific inhibitor of complex II (*Ethe1*$^{+/+}$ animals [Fig. 5D]; *Ethe1*$^{-/-}$ animals [Fig. 5E]), or (ii) without succinate, the specific substrate of SDH (*Ethe1*$^{+/+}$ animals [Fig. 5F]; *Ethe1*$^{-/-}$ animals [Fig. 5G]). As expected, the *Ethe1*$^{+/+}$ muscle displayed the normal pattern in standard SDH protocol, but developed hardly any staining in the presence of malonate or in the absence of succinate, indicating that the reaction was indeed specific to SDH. However, the *Ethe1*$^{-/-}$ muscle sections still turned deep blue in the presence of the SDH inhibitor (malonate) or in the absence of the reducing substrate (succinate). A blank reaction performed by omitting NBT failed to stain both *Ethe1*$^{+/+}$ (Fig. 5H) and *Ethe1*$^{-/-}$ muscle specimens (Fig. 5I). Taken together, these results indicate that (i) H_2S is capable of directly reducing tetrazolium into formazan and (ii) the deep-blue staining observed in *Ethe1*$^{-/-}$ muscle is, at least partly, independent of SDH activity.

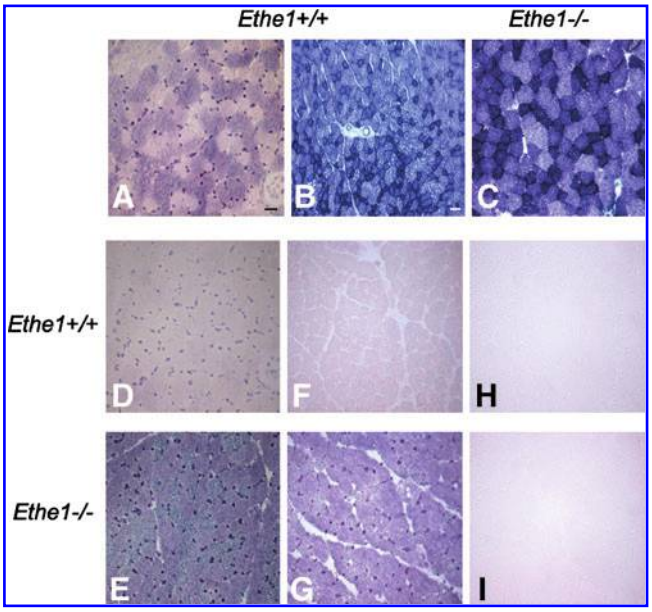

FIG. 5. SDH histochemistry on muscle sections under different conditions. Standard SDH reaction is shown on muscle sections of *Ethe1*$^{+/+}$ and *Ethe1*$^{-/-}$ animals. Addition or elimination of specific compounds (see the Materials and Methods section) in the standard SDH incubation mixture are indicated. **(A)** Standard SDH reaction on *Ethe1*$^{+/+}$ muscle. **(B)** Standard SDH reaction with addition of 1 m*M* NaHS on *Ethe1*$^{+/+}$ muscle. **(C)** Standard SDH reaction on muscle of *Ethe1*$^{-/-}$ mice. **(D)** Sodium malonate (10 m*M*), an SDH inhibitor, was added to the incubation medium of standard SDH reaction on *Ethe1*$^{+/+}$ muscle. **(E)** Sodium malonate (10 m*M*), an SDH inhibitor, was added to the incubation medium of standard SDH reaction on *Ethe1*$^{-/-}$ muscle. **(F)** SDH reaction was performed without succinate on *Ethe1*$^{+/+}$ muscle. **(G)** SDH reaction was performed without succinate on *Ethe1*$^{-/-}$ muscle. **(H)** SDH reaction was performed without nitro blue tetrazolium on *Ethe1*$^{+/+}$ muscle. **(I)** SDH reaction was performed without nitro blue tetrazolium on *Ethe1*$^{-/-}$ mice muscle. NaHS, sodium hydrosulfide. (To see this illustration in color the reader is referred to the web version of this article at www.liebertonline.com/ars).

Evaluation of COX expression

To understand the mechanism of COX deficiency in EE, we performed Western blot immunovisualization on several COX subunits in the liver, muscle, and brain homogenates of constitutive *Ethe1*$^{-/-}$ mice at different ages (P14, P21, and P30). The amount of the mtDNA-encoded MTCO1 subunit decreased progressively over time in muscle and brain, but not in the liver (Fig. 6A). The same phenomenon was observed for the nucleus-encoded subunits of COX; for instance, hardly any COX4-specific cross-reacting material was detectable in muscle at P30; subunit 5A was also decreased, in the same tissue, though to a lesser extent (Fig. 6A). Therefore, the reduction of nuclear and mitochondrial-encoded COX subunits seems to be time dependent, according to a mechanism associated with chronic, progressive accumulation of H_2S in critical tissues, and are in excellent agreement with the progressive reduction of COX activity.

The same reduction of subunits MTCO1 and COX5A was observed in muscle of the Myo-D specific *Ethe1*$^{-/-}$ conditional model, and in the brain of the nestin-specific model. No reduction was observed in the liver, muscle, or brain of the liver-specific *Ethe1*$^{-/-}$ animals (Fig. 6B).

The decrease in the amount of single COX subunits reflects a parallel decrease of steady-state COX holoenzyme. What is the mechanism underpinning this phenomenon? A first possibility is reduced expression of COX-encoding genes. This hypothesis was ruled out by real-time quantitative PCR analysis in different tissues of WT and *Ethe1*$^{-/-}$ animals. We found no differences in the transcript level for MTCO1, MTCO2, COX4, and COX5A, indicating that the decrease in the amount of COX subunits and holoenzyme occurs post-transcriptionally (Fig. 6C). A second possibility is impaired translation and assembly, and a third is accelerated degradation of COX.

To test these hypotheses, we performed mitochondrial *in vivo* pulse-chased translation assay in primary human fibroblasts exposed to NaHS. The pulse experiment, in which mitochondrial translation is allowed to proceed for 2 h, evaluates the capacity of NaHS to affect the *de novo* synthesis of mitochondrial proteins, whereas the chase experiment, which follows the persistence of radiolabeled proteins over a prolonged period (24 h), explores the effects of NaHS on protein

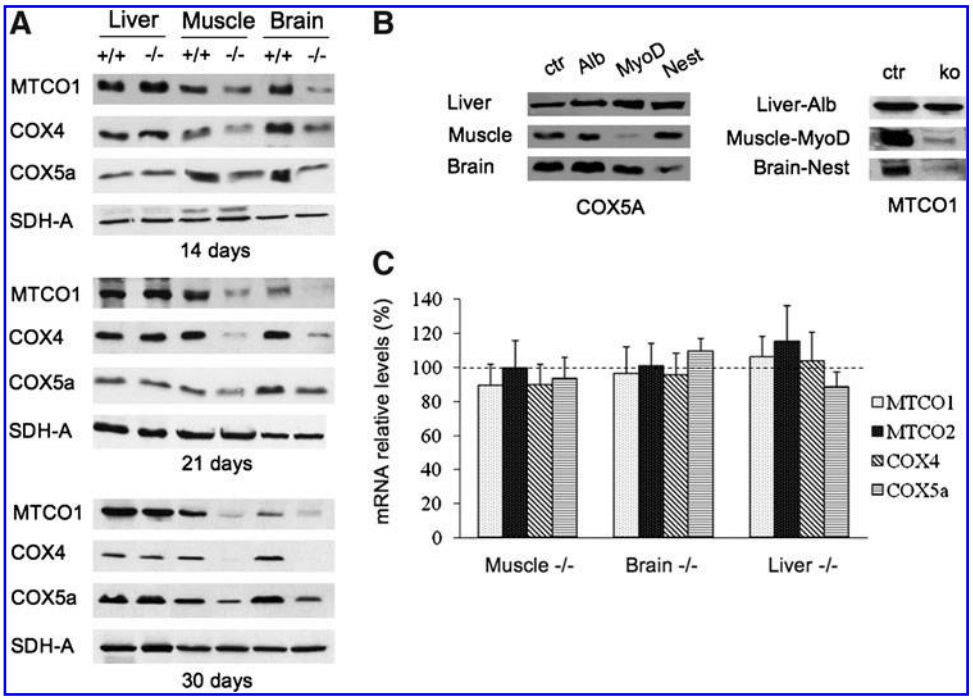

FIG. 6. COX expression in mouse tissues. (A) Western blot analysis of COX protein subunits in the liver, muscle, and brain of constitutive *Ethe1*$^{-/-}$ mice at different ages (P14, P21, and P30). **(B)** Western blot analysis using α-COX5A in different tissues of MyoD, nestin, and albumin-conditional *Ethe1*$^{-/-}$ mice; α-MTCO1 was used only in tissues specifically targeted for *Ethe1* gene ablation. ctr: *Ethe1*$^{+/+}$ mouse (WT); ko: conditional *Ethe1*$^{-/-}$ mouse (*Ethe1* knockout in the liver, muscle, and brain). **(C)** Real-time quantitative PCR analysis of COX transcripts in the liver, muscle, and brain of *Ethe1*$^{-/-}$ mice at P30. Dashed line indicates the expression level of the RNAse P control transcript. MTCO, mitochondrially encoded cytochrome c oxidase.

stability. As shown in Figure 7, the pulse experiment showed no difference in mitochondrial *de novo* protein synthesis in the absence or presence of NaHS. In contrast, the chase experiment showed a strong reduction in the amount of COX-specific subunits in cells exposed to NaHS as compared to untreated cells, clearly suggesting accelerated degradation.

Likewise, Western blot analysis performed on HeLa cells showed that the amount of cross-reacting material specific to COX1, 2, 4, and 5A decreased in a dose- and time-dependent manner, and COX4 underwent partial proteolytic degradation (Fig. 8A). These effects were specific to COX, since no decrease in the amount of either complex I (*i.e.,* NDUFA9) or complex III (*i.e.,* RISP) subunits was detected in either experiment, and the corresponding holocomplexes were both normal as demonstrated by measuring their biochemical activity (1). COX activity in NaHS-treated cells after 24 h was decreased, in parallel with the reduction in COX amount (Fig. 8B). Again, the transcript levels for COX1, 2, 4, and 5A were similar to those of untreated cells (Fig. 8C).

Recovery of COX activity in tissue homogenates exposed to NaHS

Biochemical activity of COX was spectrophotometrically measured after incubating liver, muscle, and brain homogenates with 10 μM NaHS and then leaving them exposed to air for as long as 1 h. As shown in Figure 9, COX activity progressively recovered over time, since after 30 min, COX activity reached 98% of the normal activity in the liver, 64% in muscle, and 49% in brain, indicating different efficiency of the three tissues in detoxifying H_2S.

Discussion

COX is the terminal enzyme of the mitochondrial RC, catalyzing the electron transfer from reduced cytochrome c to molecular oxygen. According to the bovine enzyme structure, mammalian complex IV is a heteromeric complex composed of 13 different subunits. The catalytic core of the enzyme consists of MTCO1 and MTCO2, two mtDNA-encoded subunits that contain the two *heme a* moieties (*a* and *a3*), and the two copper centers (Cu_A and Cu_B) responsible for electron transfer. A third mtDNA-encoded subunit (MTCO3) is part of the structural core and may play a role in proton pumping. The remaining 10 subunits (COX4; COX5A, B; COX6A, B, C; COX7A, B, C; and COX8) are encoded by nuclear genes and must be imported, processed, and assembled together with the mtDNA-encoded subunits. The function of these subunits is currently unknown, but they plausibly regulate the activity and stability of the complex. COX deficiency is a frequent cause of disease in humans, being associated with different clinical syndromes and a spectrum of gene defects (9). We demonstrated that a new pathogenic mechanism is at work in EE, based on H_2S-mediated poisoning of COX.

Since COX catalyses the oxidation of ferrocytochrome c by gaseous molecular oxygen, it is not surprising that other gases, such as NO, CO, and H_2S, can also interact with this enzyme. However, while at high concentration these gases inhibit COX activity, in trace amounts they play a

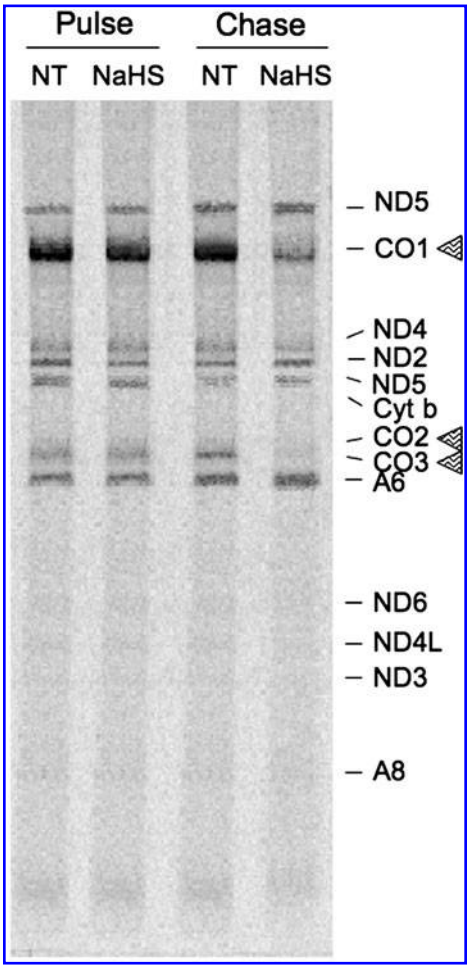

FIG. 7. Mitochondrial *in vivo* translation. mtDNA-specific protein synthesis in fibroblasts in the absence (nontreated, NT) or presence of 0.5 m*M* NaHS. Pulse experiment is reported on the left; chase experiment on the right. The autoradiographic bands are labeled according to molecular weight and to standard nomenclature: ND1, ND2, ND3, ND4, ND4L, ND5, and ND6 are subunits of cI; Cyt b is cytochrome b, a subunit of cIII; CO1, CO2, and CO3 are subunits of cIV; and A6 and A8 are subunits of cV (see www.mitomap.org/MITOMAP/MitoPolypeptide). *Arrows* indicate the absence of MTCO1, MTCO2, and MTCO3.

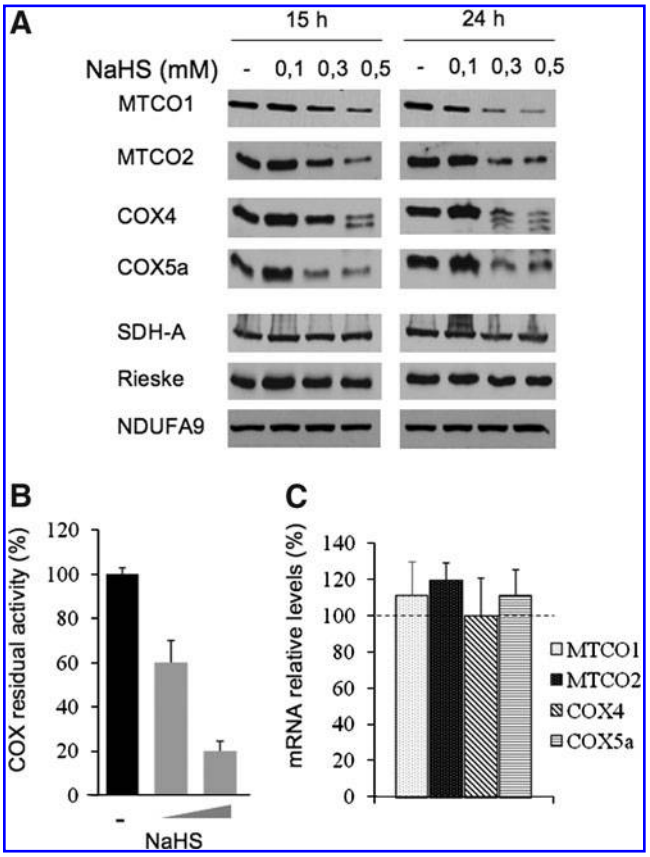

FIG. 8. COX expression in cells. (A) Western blot analysis of COX protein subunits in HeLa cells treated for 15 or 24 h with different concentration (0.1, 0.3, and 0.5 m*M*) of NaHS. **(B)** COX residual activity in HeLa cells treated with increasing concentration of NaHS (gray bars) or untreated (black bar). **(C)** Real-time quantitative PCR analysis of COX transcripts in HeLa cells treated with 0.5 m*M* NaHS for 24 h. Values are expressed as percentage (%) relative to the mean values of two standard transcripts, HPRT and GAPDH, taken as 100% (*dashed line*). See Materials and Methods section for details.

physiological role as signaling molecules and are in fact produced by normal tissues (22). H_2S, which is endogenously released from L-cysteine by either cystathionine beta-synthase or cystathionine gamma-lyase (5–26), has been proposed to regulate the vascular tone, myocardial contractility, neurotransmission, and insulin secretion.

We have demonstrated here that the ablation of *Ethe1* restricted to muscle or brain is clearly associated with an isolated COX deficiency in the targeted tissue, but not in other *Ethe1*-competent tissues. These data unequivocally demonstrate that failure to neutralize the endogenous production of H_2S is sufficient for COX activity to decrease, but not for the animals to become sick, nor for thiosulfate, an EE biomarker of H_2S levels, to increase. This observation suggests that multiorgan accumulation of H_2S and diffusion of exogenously released H_2S from the bacterial flora (1–18) are both needed to determine the severe metabolic impairment and the fatal clinical course of Ethe1-less mice and humans. Acute exposure to NaHS for just a few minutes is sufficient to inhibit COX, but this phenomenon is reversible and normal activity can be restored by competitive displacement operated by the

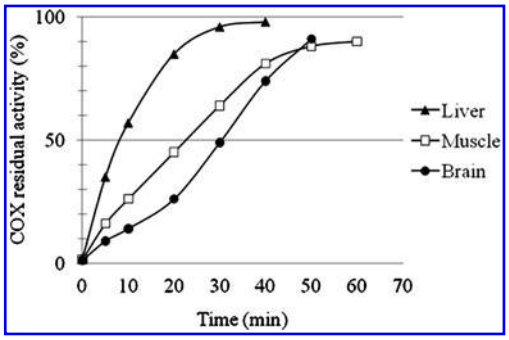

FIG. 9. Biochemical activity of COX in the presence of NaHS. Recovery of COX activity in the liver, muscle, and brain homogenates assayed at different time points after the addition of 10 μM NaHS.

oxygen contained in the air. Previous studies have shown that isolated COX is in fact reversibly inhibited by H_2S with a Ki of 0.2 μM, which is independent of oxygen concentration (20). In addition, respiration of isolated mitochondria is 50% reduced at 10 μM H_2S (33), and that of intact cells at about 30 μM (17). H_2S can also interact with the enzyme substrate, cytochrome c, and reduce it (19). However, we showed that, besides direct COX inhibition, chronic exposure to H_2S elicits a time- and dosage-dependent decrease in the amount of the holoenzyme, making the defect permanent and irreversible. Taken together, these findings indicate that in spontaneous and experimental EE the chronic exposure to high levels of H_2S causes a progressive intoxication of tissues, due to a variety of effects, including COX deficiency.

Since COX-specific transcription was normal in *Ethe1*$^{-/-}$ tissues and NaHS-treated cells, the decrease of COX holoenzyme must be due to either defective assembly or accelerated degradation of the enzyme. While the former possibility is unlikely, since assembly intermediates, which are usually observed in defects of COX assembly, were consistently absent in *Ethe1*$^{-/-}$ tissues (30), the concordant decrease of both COX holoenzyme and individual subunits, demonstrated by *in vitro* translation assay and Western blot analysis, indicates accelerated degradation of a (crippled) enzyme.

What is the mechanism underlying this phenomenon? COX inhibition by H_2S is exerted on the oxidized states of the binuclear center of the enzyme; in the fully inhibited state, COX captures two sulfide molecules, one bound to reduced Cu_B and the second to oxidized heme a3 (13). An excess of sulfide maintains in a reduced-state cytochrome a, Cu_A, and Cu_B, and determines the formation of cytochrome a3-SH complex. According to a recently proposed functional COX model under conditions mimicking rate-limiting electron flux (7), at high concentrations, H_2S binds to the reduced, FeII, active metal center of heme a_3 (8), thus competing with O_2 for binding to the reduced FeIICuI active site (8). Based on our results, we propose that the binding of H_2S to the metal core causes fully assembled COX to become destabilized and get degraded, possibly starting from the protein backbone that forms its catalytic core. Accordingly, we observed stronger reduction in the amount of MTCO1, MTCO2, COX4, and COX5A, which are the first subunits to be incorporated in the nascent holoenzyme during the assembly process, together with the metal-containing moieties. We also observed the same accelerated COX degradation in normal human cells chronically treated with H_2S. Similar to that observed in mouse tissues, COX deficiency was associated with reduction in the protein amount of subunits MTCO1, MTCO2, COX4, and COX 5A, but transcription of the corresponding genes was normal. Importantly, no other RC complex appeared to be affected, although other enzymatic activities, not directly correlated with the function of the RC, are also likely to be inhibited by sulfide.

A baffling observation is that, despite the presence of elevated sulfide concentrations, COX is not inhibited in *Ethe1*$^{-/-}$ hepatocytes. In agreement with our results, Dorman *et al.* (10) observed significantly elevated, rather than reduced, COX activity in livers of rats exposed to >10 ppm H_2S for 3 h. Along the same line, Huang *et al.* (14) also observed a small, although statistically nonsignificant, increase in liver COX activity of rats exposed to 100 ppm H_2S for 8 h/day, 5 days/week, for 5 weeks. The biological significance of this observation is unclear, but our data on the conditional liver-specific *Ethe1*$^{-/-}$ mouse model also suggests that respiration in liver is not inhibited by H_2S, possibly because H_2S neutralization is carried out in this tissue by either additional or more efficient detoxifying systems. In line with this idea, we showed that the most rapid recovery of H_2S-induced COX inhibition was indeed obtained in control liver homogenate, compared with a much slower recovery of muscle and brain.

Acknowledgments

This work was supported by the Pierfranco and Luisa Mariani Foundation Italy, Fondazione Telethon-Italy grant number GGP07019, and grant RF-INN-2007-634163 of the Italian Ministry of Health. The authors would like to thank the Italian Association "Amici del Centro Dino Ferrari."

Author Disclosure Statement

No competing financial interests exist.

References

1. Blachier F, Davila AM, Mimoun S, Benetti PH, Atanasiu C, Andriamihaja M, Benamouzig R, Bouillaud F, and Tomé D. Luminal sulfide and large intestine mucosa: friend or foe? *Amino Acids* 39: 335–347, 2010.
2. Bugiani M, Invernizzi F, Alberio S, Briem E, Lamantea E, Carrara F, Moroni I, Farina L, Spada M, Donati MA, Uziel G, and Zeviani M. Clinical and molecular findings in children with complex I deficiency. *Biochim Biophys Acta*. 1659: 136–147, 2004.
3. Burlina AB, Dionisi-Vici C, Bennett MJ, Gibson KM, Servidei S, Bertini E, Hale DE, Schmidt-Sommerfeld E, Sabetta G, Zacchello F, *et al.* A new syndrome with ethylmalonic aciduria and normal fatty acid oxidation in fibroblasts. *J Pediatr* 124: 79–86, 1994.
4. Chen JC, Mortimer J, Marley J, and Goldhamer DJ. MyoD-cre transgenic mice: a model for conditional mutagenesis and lineage tracing of skeletal muscle. *Genesis* 41: 116–121, 2005.
5. Chiku T, Padovani D, Zhu W, Singh S, Vitvitsky V, and Banerjee R. H2S biogenesis by human cystathionine gamma-lyase leads to the novel sulfur metabolites lanthionine and homolanthionine and is responsive to the grade of hyperhomocysteinemia. *J Biol Chem* 284: 11601–11612, 2009.
6. Chomyn A. *In vivo* labeling and analysis of human mitochondrial translation products. *Methods Enzymol* 264: 197–211, 1996.
7. Collman JP, Devaraj NK, Decréau RA, Yang Y, Yan YL, Ebina W, Eberspacher TA, and Chidsey CE. A cytochrome C oxidase model catalyzes oxygen to water reduction under rate-limiting electron flux. *Science* 315: 1565–1568, 2007.
8. Collman JP, Ghosh S, Dey A, and Decréau RA. Using a functional enzyme model to understand the chemistry behind hydrogen sulfide induced hibernation. *Proc Natl Acad Sci U S A* 106: 22090–22095, 2009.
9. DiMauro S and Schon EA. Mitochondrial respiratory-chain diseases. *N Engl J Med* 348: 2656–2668, 2003.
10. Dorman DC, Moulin FJ, McManus BE, Mahle KC, James RA, and Struve MF. Cytochrome oxidase inhibition induced by acute hydrogen sulfide inhalation: correlation with tissue sulfide concentrations in the rat brain, liver, lung, and nasal epithelium. *Toxicol Sci* 65: 18–25, 2002.
11. Furne J, Springfield J, Koenig T, DeMaster E, and Levitt MD. Detoxification of hydrogen sulfide and methanethiol in the cecal mucosa. *J Clin Invest* 104: 1107–1114, 1999.

12. Hildebrandt TM and Grieshaber MK. Three enzymatic activities catalyze the oxidation of sulfide to thiosulfate in mammalian and invertebrate mitochondria. *FEBS J* 275: 3352–3361, 2008.
13. Hill BC, Woon TC, Nicholls P, Peterson J, Greenwood C, and Thomson AJ. Interactions of sulphide and other ligands with cytochrome c oxidase. An electron-paramagnetic-resonance study. *Biochem J* 224: 591–600, 1984.
14. Huang J, Niknahad H, Khan S, and O'Brien PJ. Hepatocyte-catalysed detoxification of cyanide by L- and D-cysteine. *Biochem Pharmacol* 55: 1983–1990, 1998.
15. Kabil O and Banerjee R. The redox biochemistry of hydrogen sulfide. *J Biol Chem* 285: 21903–21907, 2010.
16. Kanki H, Suzuki H, and Itohara S. High-efficiency CAG-FLPe deleter mice in C57BL/6J background. *Exp Anim* 55: 137–141, 2006.
17. Leschelle X, Goubern M, Andriamihaja M, Blottière HM, Couplan E, Gonzalez-Barroso MD, Petit C, Pagniez A, Chaumontet C, Mignotte B, Bouillaud F, and Blachier F. Adaptative metabolic response of human colonic epithelial cells to the adverse effects of the luminal compound sulfide. *Biochim Biophys Acta* 1725: 201–212, 2005.
18. Levitt MD, Springfield J, Furne J, Koenig T, and Suarez FL. Physiology of sulfide in the rat colon: use of bismuth to assess colonic sulfide production. *J Appl Physiol* 92: 1655–1660, 2002.
19. Nicholls P and Kim JK. Sulphide as an inhibitor and electron donor for the cytochrome c oxidase system. *Can J Biochem* 60: 613–623, 1982.
20. Petersen LC. The effect of inhibitors on the oxygen kinetics of cytochrome c oxidase. *Biochim Biophys Acta* 460: 299–307, 1977.
21. Postic C, Shiota M, Niswender KD, Jetton TL, Chen Y, Moates JM, Shelton KD, Lindner J, Cherrington AD, and Magnuson MA. Dual roles for glucokinase in glucose homeostasis as determined by liver and pancreatic beta cell-specific gene knock-outs using Cre recombinase. *J Biol Chem* 274: 305–315, 1999.
22. Reiffenstein RJ, Hulbert WC, and Roth SH. Toxicology of hydrogen sulfide. *Annu Rev Pharmacol Toxicol* 32: 109–134, 1992.
23. Rowan FE, Docherty NG, Coffey JC, and O'Connell PR. Sulphate-reducing bacteria and hydrogen sulphide in the aetiology of ulcerative colitis. *Br J Surg* 96: 151–158, Review 2009.
24. Sciacco M and Bonilla E. Cytochemistry and immunocytochemistry of mitochondria in tissue sections. *Methods Enzymol* 264: 509–521, 1996.
25. Shih VE, Carney MM, and Mandell R. A simple screening test for sulfite oxidase deficiency: detection of urinary thiosulfate by a modification of Sörbo's method. *Clin Chim Acta* 95: 143–145, 1979.
26. Singh S, Padovani D, Leslie RA, Chiku T, and Banerjee R. Relative contributions of cystathionine beta-synthase and gamma-cystathionase to H2S biogenesis via alternative transsulfuration reactions. *J Biol Chem* 284: 22457–22466, 2009.
27. Szabó C. Hydrogen sulphide and its therapeutic potential. *Nat Rev Drug Discov* 6: 917–935, 2007.
28. Tiranti V, D'Adamo P, Briem E, Ferrari G, Mineri R, Lamantea E, Mandel H, Balestri P, Garcia-Silva MT, Vollmer B, Rinaldo P, Hahn SH, Leonard J, Rahman S, Dionisi-Vici C, Garavaglia B, Gasparini P, and Zeviani M. Ethylmalonic encephalopathy is caused by mutations in ETHE1, a gene encoding a mitochondrial matrix protein. *Am J Hum Genet* 74: 239–252, 2004.
29. Tiranti V, Galimberti C, Nijtmans L, Bovolenta S, Perini MP, and Zeviani M. Characterization of SURF-1 expression and Surf-1p function in normal and disease conditions. *Hum Mol Genet* 8: 2533–2540, 1999.
30. Tiranti V, Viscomi C, Hildebrandt T, Di Meo I, Mineri R, Tiveron C, Levitt MD, Prelle A, Fagiolari G, Rimoldi M, and Zeviani M. Loss of ETHE1, a mitochondrial dioxygenase, causes fatal sulfide toxicity in ethylmalonic encephalopathy. *Nat Med* 15: 200–205, 2009.
31. Tronche F, Kellendonk C, Kretz O, Gass P, Anlag K, Orban PC, Bock R, Klein R, and Schütz G. Disruption of the glucocorticoid receptor gene in the nervous system results in reduced anxiety. *Nat Genet* 23: 99–103, 1999.
32. Wilson K, Mudra M, Furne J, and Levitt M. Differentiation of the roles of sulfide oxidase and rhodanese in the detoxification of sulfide by the colonic mucosa. *Dig Dis Sci* 53: 277–283, 2008.
33. Yong R and Searcy DG. Sulfide oxidation coupled to ATP synthesis in chicken liver mitochondria. *Comp Biochem Physiol B Biochem Mol Biol* 129: 129–137, 2001.

Address correspondence to:
Dr. Massimo Zeviani
Unit of Molecular Neurogenetics
Institute of Neurology "Carlo Besta"–IRCCS Foundation
Via Temolo 4
20126 Milan
Italy

E-mail: zeviani@istituto-besta.it

Dr. Valeria Tiranti
Unit of Molecular Neurogenetics
Institute of Neurology "Carlo Besta"–IRCCS Foundation
Via Temolo 4
20126 Milan
Italy

E-mail: tiranti@istituto-besta.it

Date of first submission to ARS Central, August 2, 2010; date of acceptance, September 2, 2010.

Abbreviations Used

COX = cytochrome c oxidase
COX4 = cytochrome c oxidase subunit 4
COX5A = cytochrome c oxidase subunit 5A
CS = citrate synthase
DMEM = Dulbecco's modified Eagle's medium
EDTA = ethylenediaminetetraacetic acid
EE = ethylmalonic encephalopathy
MTCO1 = mitochondrially encoded cytochrome c oxidase 1
MTCO2 = mitochondrially encoded cytochrome c oxidase 2
NaHS = sodium hydrosulfide
NBT = nitro blue tetrazolium
NDUFA9 = NADH dehydrogenase (ubiquinone) 1 alpha subcomplex, 9
RC = respiratory chain
RISP = α-Rieske iron–sulfur protein
SDH = succinate dehydrogenase
SDO = sulfur dioxygenase
WT = wild type

This article has been cited by:

1. Ivano Di Meo, Alberto Auricchio, Costanza Lamperti, Alberto Burlina, Carlo Viscomi, Massimo Zeviani. 2012. Effective AAV-mediated gene therapy in a mouse model of ethylmalonic encephalopathy. *EMBO Molecular Medicine* **4**:9, 1008-1014. [CrossRef]
2. D. Chao, X. He, Y. Yang, G. Balboni, S. Salvadori, K. H. Dong, Y. Xia. 2012. Hydrogen sulfide induced disruption of Na + homeostasis in the cortex. *Toxicological Sciences* . [CrossRef]
3. Kenneth R. Olson. 2012. Mitochondrial adaptations to utilize hydrogen sulfide for energy and signaling. *Journal of Comparative Physiology B* . [CrossRef]
4. Carla Giordano, Carlo Viscomi, Maurizia Orlandi, Paola Papoff, Alberto Spalice, Alberto Burlina, Ivano Meo, Valeria Tiranti, Vincenzo Leuzzi, Giulia d'Amati, Massimo Zeviani. 2011. Morphologic evidence of diffuse vascular damage in human and in the experimental model of ethylmalonic encephalopathy. *Journal of Inherited Metabolic Disease* . [CrossRef]
5. Ruma Banerjee . 2011. Hydrogen Sulfide: Redox Metabolism and Signaling. *Antioxidants & Redox Signaling* **15**:2, 339-341. [Abstract] [Full Text HTML] [Full Text PDF] [Full Text PDF with Links]
6. Tatjana M. Hildebrandt. 2011. Modulation of sulfide oxidation and toxicity in rat mitochondria by dehydroascorbic acid. *Biochimica et Biophysica Acta (BBA) - Bioenergetics* . [CrossRef]